RESEARCH ARTICLE

Coaxial nozzle-assisted electrohydrodynamic printing for microscale 3D cell-laden constructs

Hongtao Liang, Jiankang He*, Jinke Chang, Bing Zhang, Dichen Li

State key laboratory for manufacturing systems engineering, Xi'an Jiaotong University, Xi'an, China

Abstract: Cell printing has found wide applications in biomedical fields due to its unique capability in fabricating living tissue constructs with precise control over cell arrangements. However, it is still challenging to print cell-laden 3D structures simultaneously with high resolution and high cell viability. Here a coaxial nozzle-assisted electrohydrodynamic cell printing strategy was developed to fabricate living 3D cell-laden constructs. Critical process parameters such as feeding rate and stage moving speed were evaluated to achieve smaller hydrogel filaments. The effect of $CaCl_2$ feeding rate on the printing of 3D alginate hydrogel constructs was also investigated. The results indicated that the presented strategy can print 3D hydrogel structures with relatively uniform filament dimension (about 80 μm) and cell distribution. The viability of the encapsulated cells was over 90%. We envision that the coaxial nozzle-assisted electrohydrodynamic printing will become a promising cell printing strategy to advance biomedical innovations.

Keywords: electrohydrodynamic printing; cell printing; bioprinting; biofabrication; tissue engineering

*Correspondence to: Jiankang He, State Key Laboratory for Manufacturing Systems Engineering, Xi'an Jiaotong University, Xi'an 710049, China; jiankanghe@mail.xjtu.edu.cn

Received: October 1, 2017; **Accepted**: November 13, 2017; **Published Online**: November 22, 2017

Citation: Liang H, He J, Chang J, *et al*., 2018, Coaxial nozzle-assisted electrohydrodynamic printing for microscale 3D cell-laden constructs. *Int J Bioprint*, 4(1): 127. http://dx.doi.org/10.18063/IJB.v4i1.127

1. Introduction

In the past decades, cell printing has been extensively studied in biomedical fields due to its unique capability in precise patterning of biological components such as living cells in a controlled manner[1–3]. Several bioprinting techniques have been developed mainly including microextrusion-based printing, inkjet printing and laser-assisted printing[4–6]. However, there are some drawbacks of these existing strategies in fabricating complex three-dimensional (3D) structures with relatively high resolution and high cell viability in a costly effective way. For example, inkjet cell printing employs thermal or piezoelectric effect to print cell-hydrogel droplets, which affects cell viability and limits low cell concentration[4,7]. Laser-assisted printing commonly requires costly equipment and cannot fabricate 3D constructs[6,8]. Microextrusion-based cell printing has the drawbacks of low printing resolution as well as the side effect of flow-induced shear stress on cell viability[9–11].

Electrohydrodynamic jetting or printing recently attracts extensive attentions in fabricating high-resolution features based on the principle of electrohydrodynamically induced material flows[12–18]. Several process parameters had been investigated to achieve stable electrohydrodynamic printing process, such as applied voltage, moving speed, feeding rate of materials and inter diameter of nozzle[19–26]. Recent explorations indicate that biomaterials like living cells and hydrogels can be electrohydrodynamically printed and maintained their viability[27–30]. For example, Gasperini *et al*. further fabricated hollow cylindrical cell-laden structures using an electrohydrodynamic bioprinter[31]. Yao *et al*. fabricated 3D cell-laden alginate structures with the help of aerosol crosslinking mechanism by combining electrohydrodynamic printing and traditional extrusion-based cell printing[32]. However, the size of these electrohydrodynamically printed hydrogel filaments was commonly larger than 200 μm.

We previously developed a novel electrohydrodynamic cell printing strategy that can fabricate cell-laden constructs with microscale resolution (<100 μm) and high cell viability (>95%)[33]. However, alginate filaments were mainly crosslinked by the calcium ions diffused from the collecting substrate of agarose hydrogel, which limited the layer number of the electrohydrodynamically printed hydrogel smaller than 20. Here a coaxial nozzle-

assisted electrohydrodynamic cell printing process was further presented aiming to fabricate 3D cell-laden constructs with high resolution and high cell viability. The printed alginate filament can be instantly crosslinked by the calcium chloride solution flowed from the coaxial nozzle during the 3D electrohydrodynamic printing process.

2. Materials and Methods

2.1 Materials

Alginate with medium viscosity (2000 mPa·s) was purchased from Sigma (United Kingdom). Calcium chloride powder was bought from Aladdin (Shanghai, China). Agarose powder with low melting temperature (87–89 °C) was bought from Biowest (Spain). 3% (w/v) alginate solution was prepared by dissolving alginate powder into phosphate buffer saline (PBS). 2% (w/v) agarose solution with 3% (w/v) calcium chloride was prepared by dissolving agarose and calcium chloride powders in tris-buffered saline (TBS) at 100 °C. 1% (w/v) calcium chloride solution was prepared by dissolving calcium chloride powder into TBS at room temperature. Flat agarose hydrogel with a thickness of 3 mm was prepared by casting agarose solution in a petri dish. For electrohydrodynamic cell printing, rat myocardial cell lines (H9C2, ATCC) were added into alginate solution with a density of 1×10^6 cells mL^{-1}.

2.2 Coaxial Nozzle-Assisted Electrohydrodynamic Cell Printing Platform

A house-made electrohydrodynamic printing platform was used which mainly consists of three components: a high-voltage generator (ZGF-30/5, Welldone, Shanghai, China), a multi-channel syringe pump system (TJ-2A, Longer Pump, Baoding, China) and a high-resolution x-y-z movement stage (Xiamen Heidelstar Co., China). Alginate solution and calcium chloride solution were loaded into two 1 mL syringes which were separately controlled by the syringe pump. A coaxial printing nozzle was mounted onto the z-axis and connected with the positive terminal of a high-voltage generator. The core inlet of the nozzle was connected with the syringe loaded with alginate solution while the sheath inlet of the nozzle was connected with the syringe loaded with calcium chloride solution respectively *via* soft tubes as shown in Figure 1. Insulating petri dish and agarose hydrogel with calcium ions were sequentially placed on the grounded x-y moving stage as the collecting substrate. The distance between the coaxial nozzle and the collecting substrate was fixed at 200 μm.

To initialize the electrohydrodynamic printing process, high voltage was applied and the syringe pump was opened to simultaneously feed alginate solution and calcium chloride solution into the coaxial nozzle. The electrohydrodynamically printed alginate solution was instantly crosslinked in contact with calcium chloride solution to form hydrogel filaments and deposit onto the collecting substrate. The deposition of alginate hydrogel filaments could be flexibly controlled to fabricate complex patterns by directing the movement of x-y stage according to a user-specific design. A 3D hydrogel structure can be further electrohydrodynamically printed by precisely stacking the alginate filaments in a layer-by-layer manner.

2.3 Effect of Applied Voltage on the Width of the Printed Filaments

To tightly attach the printed hydrogel filament to the collecting substrate, calcium chloride solution was not supplied in the printing of the first three layers. The electrohydrodynamically printed alginate filament was crosslinked by the calcium ions in agarose hydrogel.

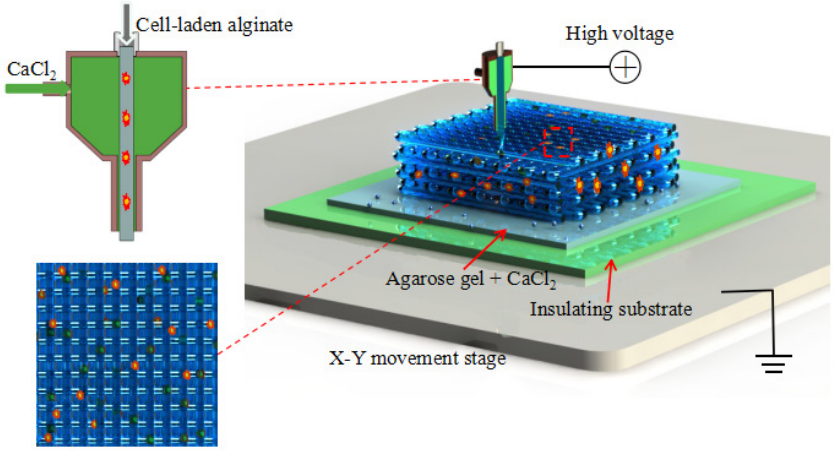

Figure 1. Schematic of coaxial nozzle-assisted electrohydrodynamic printing for microscale cell-laden constructs

We firstly compared the width of the printed filaments with or without applied voltage under different nozzle diameter when alginate feeing rate and stage moving speed were fixed at 600 μL/h and 15 mm/s, respectively. Three kinds of coaxial nozzles were used with the core/sheath diameter of 160/500 μm (30G/21G), 260/840 μm (25G/18G) and 410/1010 μm (22G/17G). The morphology and width of the printed filaments were characterized with an inverted fluorescence microscope (ECLIPSE Ti, Nikon, Japan). For each condition, three samples were separately printed with nine locations totally measured.

2.4 Effect of Process Parameters on the Width of Electrohydrodynamically Printed Filaments

The effect of alginate feeding rate and stage moving speeding on the width of the electrohydrodynamically printed filaments was studied when the applied voltage and nozzle-to-substrate distance were fixed at 4.5 kV and 200 μm. Alginate feeding rate of gradually increased from 200 μL/h to 1000 μL/h when the stage moving speed was fixed at 30 mm/s. The moving speed changed from 15 mm/s to 35 mm/s when alginate feeding rate was fixed at 400 μL/h. The morphology of the printed filaments was characterized and the filament width was expressed as mean ± standard deviation.

2.5 Effect of $CaCl_2$ Feeding Rate on the Electrohydrodynamic Printing of 3D Constructs

To fabricate 3D hydrogel constructs using the presented electrohydrodynamic printing method, it is necessary to simultaneously feed alginate and $CaCl_2$ solutions using the coaxial nozzle to ensure instant crosslinking when the layer number is over 3. The effect of $CaCl_2$ feeding rate on the maximum layer number of the printed constructs was investigated. $CaCl_2$ feeding rate varied in the range of 0–300 μL/h and the maximum layer number was recorded when the electrohydrodynamic printing process became unstable.

2.6 Characterization of the Electrohydrodynamically Printed 3D Hydrogel Constructs

3D hydrogel constructs with different layer number of 10, 30, 50 and 70 were electrohydrodynamically printed. The macro/microscopic images of the resultant constructs were viewed with a digital camera (Nikon, Japan) or optical microscope. The 3D profiles of the printed constructs were reconstructed using a confocal laser scanning microscope (OLS4000, Olympus, USA), based on which the construct height was quantified. The electrohydrodynamically printed constructs with 50 layers were further freeze-dried in a lyophilizer (FD-1A-50, Biocool, Beijing, China) for three days. The microstructures were observed with scanning electron microscope (SEM, SU8010, Hitachi, Japan).

2.7 Electrohydrodynamic Printing of 3D Cell-Laden Constructs

To demonstrate the capability of the presented strategy for cell printing, 3D cell-laden constructs with a layer number of 30 were electrohydrodynamically printed. To evaluate cell viability, Live/Dead assay (Thermo Fisher Scientific, USA) was performed according to the manufacture's specifications. The 3D fluorescent images of the constructs were reconstructed with a confocal microscopy (Nikon, Japan). Cell number and cell viability at specific layer of 5, 15 and 25 were quantified. The quantified data is expressed as mean ± standard deviation. Statistical analysis was performed using analysis of variance in Microsoft Excel software. Values of $p < 0.05$ was considered to be statistically significant.

3. Results and Discussion

Figure 2A–F show the morphology of alginate filaments electrohydrodynamically printed by different nozzle diameter without/with applied voltage. When the voltage was not applied, the width of the printed filaments gradually increased from 166.15 ± 2.67 μm to 196.78 ± 4.87 μm as the core nozzle diameter changed from 160 μm to 410 μm. When the voltage of 4.5 kV was applied, the width of the electrohydrodynamically printed filaments increased from 144.24 ± 4.82 μm to 167.33 ± 7.40 μm as the nozzle diameter increased. In all cases, the width of the electrohydrodynamically printed filaments was obviously smaller than that of extrusion-based printing filaments as shown in Figure 2G. This indicated that applied voltage could decrease the width of the printed filaments. Previous studies also indicated that a thinner Taylor cone could be achieved under a higher voltage, which can decrease line width during the printing process[19,20]. Therefore, in the following experiment, applied voltage of 4.5 kV and the coaxial nozzle with core diameter of 160 μm and sheath diameter of 500 μm were used to achieve relatively smaller filaments.

Figure 3A shows the filament morphology as well as the measured width of the electrohydrodynamically printed filaments under fixed stage moving speed of 30 mm/s and different alginate feeding rate. When the alginate feeding rate was lower than 400 μL/h, the printed filaments were discontinuous. As the alginate feeding rate increased from 400 μL/h to 1000 μL/h, the filament width significantly increased from 92.53 ± 2.75 μm to 137.70 ± 2.99 μm. When alginate feeding rate was fixed at 400 μL/h, the printed filament was straight and continuous and the filament width significantly decreased from 122.24 ± 4.42 μm to 92.53 ± 2.75 μm as

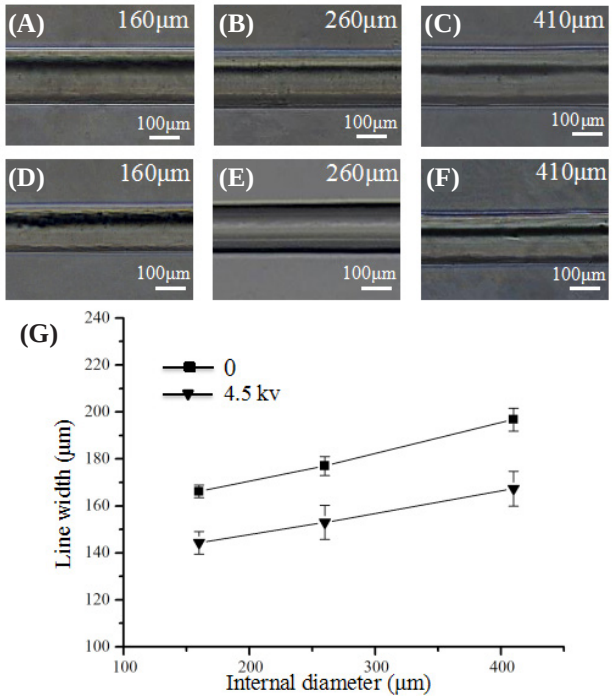

Figure 2. Effect of high voltage on width of electrohydrodynamically printed filament. (**A**–**C**) Morphology of the extruded filaments as the core nozzle diameter changed from 160 μm to 410 μm. (**D**–**E**) Morphology of the electrohydrodynamically printed filaments with the voltage of 4.5 kV as the core nozzle diameter changed from 160 μm to 410 μm. (**G**) Quantification of the width of the printed filament.

stage moving speed changed from 10 mm/s to 30 mm/s in Figure 3B. When the moving speed was over 30 mm/s, the printing filaments became discontinuous. The smallest filament (<100 μm) was achieved when the feeding rate of alginate and stage moving speed were fixed at 400 μL/h and 30 mm/s, respectively.

To test the feasibility of using coaxial nozzle-assisted electrohydrodynamic printing to fabricate 3D hydrogel constructs, multilayer structures were further printed with $CaCl_2$ feeding rate of 300 μL/h after the first three layers were completed. However, it was found that the electrohydrodynamic printing process became unstable with discontinuous alginate filaments when the stage moving speed was 30 mm/s (Supplementary Movie 1). Continuous alginate filaments can be achieved when the stage moving speed decreased to 15 mm/s (Supplementary Movie 2). This was mainly caused by the flow of $CaCl_2$ solution during the electrohydrodynamic printing process. Therefore, a lower stage moving speed of 15 mm/s was used to print the 3D constructs.

The effect of $CaCl_2$ feeding rate on the electrohydrodynamic printing of 3D constructs was investigated. Figure 4A shows the microscopic images of the printed constructs with a layer number of 13 when $CaCl_2$ feeding rate is zero. It was obviously observed that the printed alginate solution was not instantly crosslinked at the top layer due to diffusion-based limitation of calcium ions and was prone to form aggregates at the crossed sites. When $CaCl_2$ feeding rate increased from 100 μL/h to 300 μL/h, more layers of alginate filaments could be electrohydrodynamically printed as shown in Figure 4B–D. The printing layer number was mainly determined by $CaCl_2$ feeding rate. Figure 4E shows the relationship between the maximum printing layer and $CaCl_2$ feeding rate. Alginate hydrogel constructs with the maximum printing layer number of 73 can be fabricated when $CaCl_2$ feeding rate was fixed at 300 μL/h. In addition, calcium chloride solution could fill in the pore of the 3D constructs as the layer number increased. Therefore, the printed cell-laden filaments were always immersed into the liquid environment during the electrohydrodynamic printing process, which might reduce the side effect of water evaporation on the cell viability.

3D alginate hydrogel constructs with different layer number were electrohydrodynamically printed when alginate feeding rate, stage moving speed and $CaCl_2$ feeding rate were fixed at 400 μL/h, 15 mm/s and 300

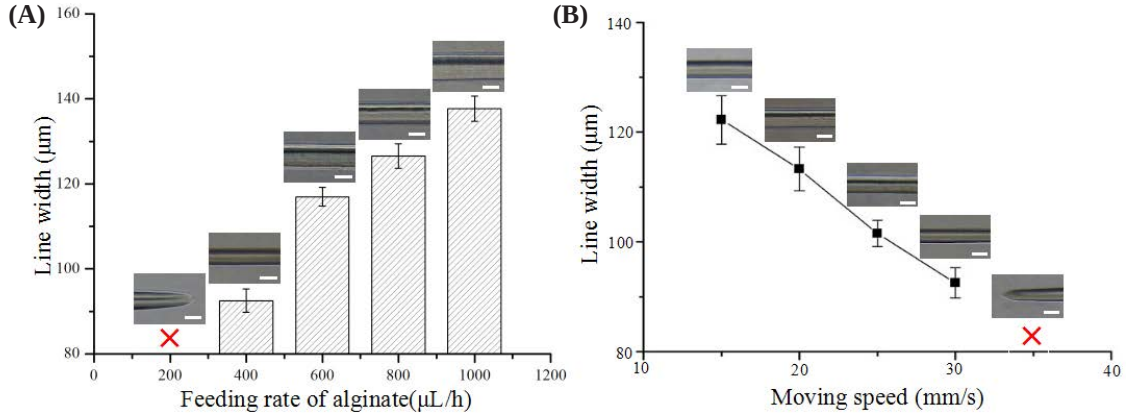

Figure 3. Effect of process parameters on the width of the electrohydrodynamically printed filaments. (**A**) Quantification of filament width as alginate feeding rate changed from 200 μL/h to 1000 μL/h. (**B**) Quantification of filament width as stage moving speed changed from 15 mm/s to 35 mm/s.

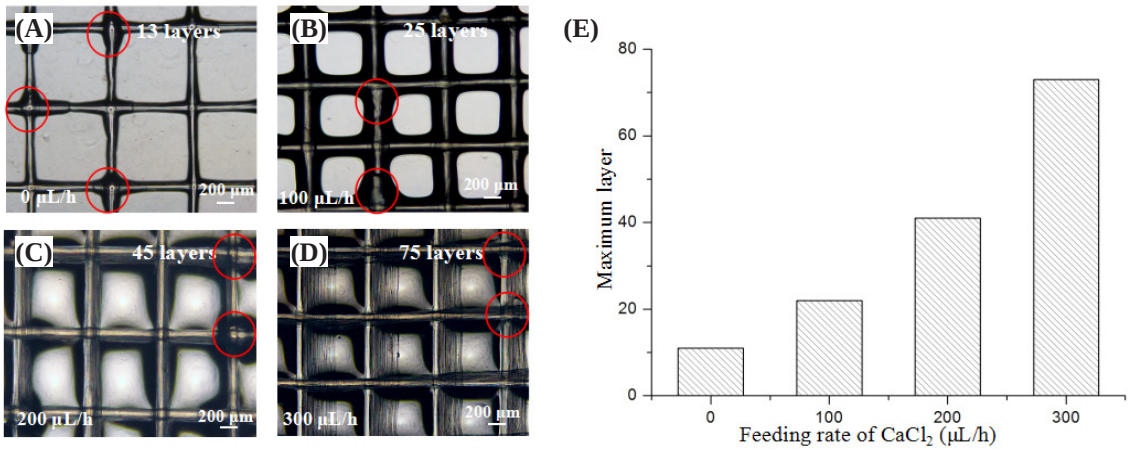

Figure 4. Effect of $CaCl_2$ feeding rate on the maximum printing layer number of the 3D constructs. (**A**–**D**) Microscopic images of the printed constructs with a layer number of 13, 25, 45 and 75 in corresponding to $CaCl_2$ feeding rate of zero, 100 μL/h, 200 μL/h and 300 μL/h. (**E**) The relationship between maximum printing layer number and $CaCl_2$ feeding rate.

μL/h, respectively. Figure 5A–D show the printed structures with the layer number of 10, 30, 50 and 70. The thickness of the printed constructs significantly increased as the layer number increased. This indicated that the electrohydrodynamically printed alginate from the core nozzle can be instantly crosslinked by calcium ions from the sheath nozzle to form tiny filaments with a relatively uniform diameter of 80 μm. In addition, the calcium chloride solution around the hydrogel filaments can significantly decrease the evaporation of water inside printed constructs, which might be important for cell viability. Figure 5E–H show the 3D profiles of the electrohydrodynamically printed constructs with the layer number of 10, 30, 50 and 70. The printed filaments were successfully stacked up to form 3D constructs in a layer-by-layer manner. The measured height for the printed constructs increased from 172.73 ± 9.93 μm to 1464.53 ± 14.46 μm as the layer number increased from 10 to 70 (Figure 5I). In all cases, the average height for each layer was about 18.53 ± 1.32 μm, which

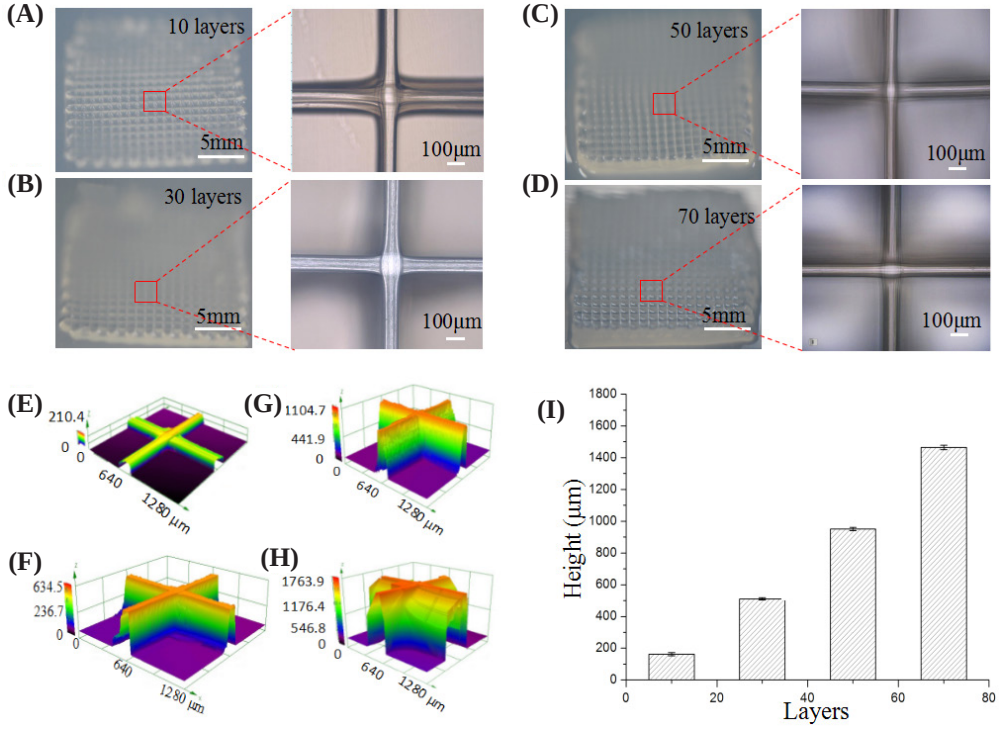

Figure 5. Electrohydrodynamic printing of 3D constructs with different layer number. (**A**–**D**) Photos and microscopic images of the constructs with the layer number of 10, 30, 50 and 70. (**E**–**H**) 3D profiles of the printed constructs with the layer number of 10, 30, 50 and 70. (**I**) Quantification of the construct height with different layer number.

further verified that the printed alginate solution could be instantly crosslinked to form hydrogel filament with uniform dimension. Since the height of each layer was close to the size of living cells, it might enable to print the filaments with single layer of cells in the vertical direction for high-resolution cell printing.

Figure 6 shows the SME images of the electrohydrodynamically printed hydrogel construct with a layer number of 50. The printed filaments at neighbor layers were tightly merged together, which maintained structural integrity after freeze drying. The diameter of the freeze-dried filaments was about 70 μm, slightly smaller than that of the freshly printed hydrogel filaments due to shrinking during the freeze-drying process. Together, these results indicated that the introduction of coaxial nozzle in the electrohydrodynamic printing process significantly enhance the capability to fabricate 3D hydrogel constructs.

Cell-laden hydrogel constructs with a layer number of 30 were finally electrohydrodynamically printed as shown in Figure 7A. Figure 7B shows fluorescent images of the cell-laden constructs (top view) stained with Live/Dead assay. The cells were completely confined inside the hydrogel filaments and most cells kept alive (green).

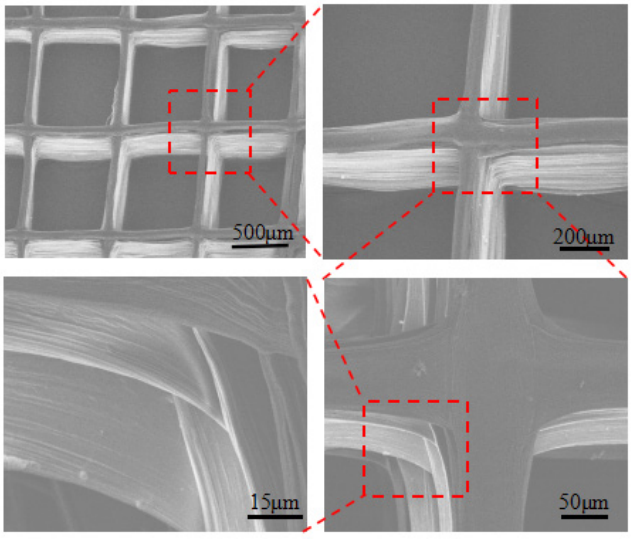

Figure 6. SEM images of the electrohydrodynamically printed construct with a layer number of 50 after freeze drying

Figure 7C illustrates the 3D profile of the printed cell-laden constructs. The height of the obtained structure was about 500 μm. Figure 7D–F show cell distribution at specific layer of 5, 15 and 25, respectively. The electrohydrodynamically printed cells were uniformly distributed among layers (p = 0.26) and the average cell number for each layer was about 70 (Figure 7G). There is no significant difference in cell viability among layers as shown in Figure 7H (p = 0.20). The cell viability was higher than 90%. These results indicated that the coaxial nozzle-assisted electrohydrodynamic printing strategy could effectively fabricate the 3D cell-laden constructs with high resolution, uniform cell distribution and high cell viability.

4. Conclusion

In summary, coaxial nozzle-assisted electrohydrodynamic printing technique was successfully developed to fabricate microscale 3D cell-laden alginate constructs. Process parameters such as applied voltage, alginate feeding rate, stage moving speed and $CaCl_2$ feeding rate were systematically studied to stably print microscale hydrogel filaments with 2D/3D organizations. 3D hydrogel constructs with the maximum layer number of 73 can be electrohydrodynamically printed in a layer-by-layer manner. The height of the printed constructs was approximately 1464.53 ± 14.46 μm and the filament dimension maintained relatively uniform (80 μm in width and 18.5 μm in height). Cell-laden constructs with uniform cell distribution and high cell viability (>90%) was finally achieved. However, it is still challenging to fabricate higher complex heterogeneous 3D living constructs with multiple cell types and hydrogel compositions. In addition, the presented coaxial nozzle-assisted electrohydrodynamic printing should be further explored to solve these problems.

Conflict of Interest and Funding

No conflict of interest was reported by the authors. This work was supported by the National Natural Science Foundation of China (51422508, 51675412), Shaanxi Key Research and Development Program (2017ZDXM-GY-058) and the Fundamental Research Funds for the Central Universities.

References

1. Kang H-W, Lee S J, Ko I K, *et al.*, 2016, A 3D bioprinting system to produce human-scale tissue constructs with structural integrity. *Nat Biotechno*, 34(3): 313–319. http://dx.doi.org/10.1038/nbt.3413
2. Jordan S M, Kelly R S, Michael T Y, *et al.*, 2012, Rapid casting of patterned vascular networks for perfusable engineered three-dimensional tissues. *Nat Mater*, 11(9): 768–774. http://dx.doi.org/10.1038/nmat335733
3. Falguni P, Jinah J, Dong-Heon H, *et al.*, 2014, Printing three-dimensional tissue analogues with decellularized extracellular matrix bioink. *Nat Commun*, 5: 3935. http://dx.doi.org/10.1038/ncomms4935
4. Sean V M, Anthony A, 2014, 3D bioprinting of tissues and organs. *Nat Biotechnol*, 32(8): 773–785. http://dx.doi.org/10.1038/nbt.2958

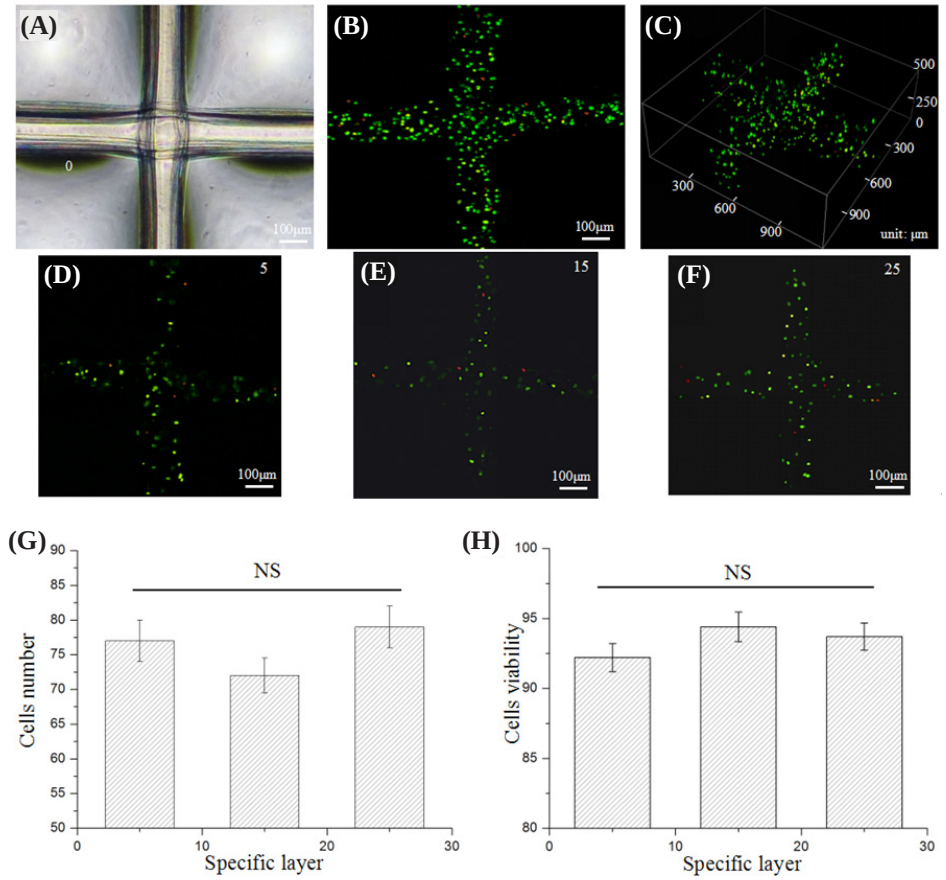

Figure 7. Electrohydrodynamic printing of 3D cell-laden constructs with a layer number of 30. (**A**) Microscopic images of the printed cell-laden constructs. (**B**–**C**) Fluorescent images (top view and 3D profile) of the electrohydrodynamically printed cell-laden constructs. (**D**–**F**) Cell distribution at specific layer of 5, 15 and 25. (**G**) Quantification of cell number at specific layer of 5, 15 and 25. (**H**) Quantification of cell viability at specific layer of 5, 15 and 25. "NS" indicates non-significance.

5. Malda J, Jetze V, Ferry P M, *et al*., 2013, 25th Anniversary article: Engineering hydrogels for biofabrication. *Adv Mater*, 25(36): 5011–5028. http://dx.doi.org/10.1002/adma.201302042
6. Thomas B, Mieke V, Jorg S, *et al*., 2012, A review of trends and limitations in hydrogel-rapid prototyping for tissue engineering. *Biomaterials*, 33(26): 6020–6041. http://dx.doi.org/10.1016/j.biomaterials.2012.04.050
7. Xu T, Zhao W Z, Zhu J M, *et al*., 2013, Complex heterogeneous tissue constructs containing multiple cell types prepared by inkjet printing technology. *Biomaterials*, 34(1): 130–139. http://dx.doi.org/10.1016/j.biomaterials.2012.09.035
8. Lothar K, Andrea D, Sabrina S, *et al*., 2012, Skin tissue generation by laser bioprinting. *Biotechnology*, 109(7): 1855–1863. http://dx.doi.org/10.1002/bit.24455
9. Zhu W, Ma X Y, Gou M L, *et al*., 2016, 3D printing of functional biomaterials for tissue engineering. *Curr Opin Biotechnol*, 40: 103–112. http://dx.doi.org/10.1016/j.copbio.2016.03.014
10. Ning LQ, Chen X B, 2017, A brief review of extrusion-based tissue scaffold bio-printing. *Biotechnol J*, 12(8): 1600671. http://dx.doi.org/10.1002/biot.201600671
11. Koo Y, Kim G, 2016, New strategy for enhancing *in situ* cell viability of cell-printing process *via* piezoelectric transducer-assisted three-dimensional printing. *Biofabrication*, 8(2): 025010. http://dx.doi.org/10.1088/1758-5090/8/2/025010
12. Zhang B, He J K, Li X, *et al*., 2016, Micro/nanoscale electrohydrodynamic printing: From 2D to 3D. *Nanoscale*, 8(34): 15376–15388. http://dx.doi.org/10.1039/c6nr04106j
13. He J K, Xu FY, Cao Y, *et al*., 2015, Towards microscale electrohydrodynamic three-dimensional printing. *J Phys D Appl Phys*, 49(5): 055504. http://dx.doi.org/10.1088/0022-3727/49/5/055504
14. He J K, Xu F Y, Dong R N, *et al*., 2016, Electrohydrodynamic 3D printing of microscale poly (ε-caprolactone) scaffolds with multi-walled carbon nanotubes. *Biofabrication*, 9(1): 015007.

http://dx.doi.org/10.1088/1758-5090/aa53bc

15. Mao M, He J K, Li X, *et al.*, 2017, The emerging frontiers and applications of high-resolution 3D printing. *Micromachines*, 8(4): 113. http://dx.doi.org/10.3390/mi8040113
16. Onses M S, Sutanto E, Ferreira P M, *et al*., 2015, Mechanisms, capabilities, and applications of high-resolution electrohydrodynamic jet printing. *Small*, 11(34): 4267–4266. http://dx.doi.org/10.1002/smll.201500593
17. Lee H, Seong B, Jang Y, *et al*., 2014, Direct alignment and patterning of silver nanowires by electrohydrodynamic jet printing. *Small*, 10(19): 3918–3922. http://dx.doi.org/10.1002/smll.201400936
18. Ahmad Z, Rasekh M, Edirisinghe M, 2010, Electrohydrodynamic direct writing of biomedical polymers and composites. *Macromol Mater Eng*, 295(4): 315–319. http://dx.doi.org/10.1002/mame.200900396
19. Parajuli D, Koomsap P, Parkhi A A, *et al*., 2016, Experimental investigation on process parameters of near-field deposition of electrispinning-based rapid prototyping. *Virtual Phys Prototyp*, 11(3):193–207. http://dx.doi.org/10.1080/17452759.2016.1210314
20. Wei C, Dong J, 2013, Direct fabrication of high-resolution three-dimensional polymeric scaffolds using electrohydrodynamic hot jet plotting. *J Micromech Microeng*, 23(2): 025017. http://dx.doi.org/10.1088/0960-1317/23/2/025017.
21. Zheng G, Sun L L, Wang X, *et al*., 2016, Electrohydrodynamic direct-writing microfiber patterns under stretching. *Appl Phys A Mater Sci Process*, 122(2): 1–9. http://dx.doi.org/10.1007/s00339-015-9584-3
22. Chanthakulchan A, Koomsap P, Parkhi, *et al*., 2015, Environmental effects in fiber fabrication using electrispinning-based rapid prototyping. *Virtual Phys Prototyp*, 10(4): 227–237. http://dx.doi.org/10.1080/17452759.2015.1112411
23. Chanthakulchan A, Koomsap P, Auyson K, *et al*., 2015, Development of an electrospinning-based rapid prototyping for scaffold fabrication, *Rapid Prototyp J*, 21(3): 329–339. http://dx.doi.org/10.1108/RPJ-11-2013-0119
24. Bisht GS, Ciulin C, Alireza M, *et al*., 2011, Controlled continuous patterning of polymeric nanofibers on three-dimensional substrates using low voltage near-field electrospinning. *Nano Lett*, 11(4): 1831–1837. http://dx.doi.org/10.1021/nl2006164
25. Li J L, Cai YL, Guo Y L, *et al*., 2014, Fabrication of three-dimensional porous scaffolds with controlled filament orientation and large pore size *via* an improved E-jetting technique. *J Biomed Mater Res B Appl Biomater*, 102B(4): 651–658. http://dx.doi.org/10.1002/jbm.b.33043
26. Bu N, Huang Y G, Wang X M, *et al*., 2012, Continuous tunable and oriented nanofiber direct-written by mechano-electrospinning. *Mater Manuf Process*, 27(12): 1318–132. http://dx.doi.org/10.1080/10426914.2012.700145
27. Jayasinghe S N, 2013, Cell electrospinning: A novel tool for functionalizing fibres, scaffolds and membranes with living cells and other advanced materials for regenerative biology and medicine. *Analyst*, 138(8): 2215–2223. http://dx.doi.org/10.1039/c3an36599a
28. Zhao X, He J K, Xu F Y, *et al*., 2016, Electrohydrodynamic printing: A potential tool for high-resolution hydrogel/cell patterning. *Virtual Phys Prototyp*, 11 (1): 57–63. http://dx.doi.org/10.1080/17452759.2016.1139378
29. Ehler E, Jayasinghe S N, 2014, Cell electrospinning cardiac patches for tissue engineering the heart. *Analyst*, 139(18): 4449–4452. http://dx.doi.org/10.1039/c4an00766b
30. Jayasinghe S N, Qureshi, A N, Eagles, P A, *et al*., 2006, Electrohydrodynamic jet processing: An advanced electric-field-driven jetting phenomenon for processing living cells. *Small*, 2(2): 216–219. http://dx.doi.org/10.1002/smll.200500291
31. Gasperini L, Manigiglio D, Motta A, *et al*., 2015, An electrohydrodynamic bioprinter for alginate hydrogels containing living cells. *Tissue Eng Part C Methods*, 21(2): 123–132. http://dx.doi.org/10.1089./ten.tec.2014.0149
32. Yeo M, Ha J H, Lee H, *et al*., 2016, Fabrication of hASCs-laden structures using extrusion-based bioprinting supplemented with an electric field. *Acta Biomater*, 38: 33–43. http://dx.doi.org/10.1016/j.actbio.2016.04.017
33. He J K, Zhao X, Chang J K, *et al*., 2017, Microscale electrohydrodynamic bioprinting with high viability. *Small*: 1702626. http://dx.doi.org/10.1002/smll.201702626